# Lowest lying $2^+$ and $3^-$ vibrational states in Pb, Sn, and Ni isotopes in relativistic quasiparticle random-phase approximation

A. Ansari
*Institute of Physics, Sainik School Post Office, Bhubaneswar 751 005, India*

P. Ring
*Physics Department, Technical University of Munich, D-85748 Garching, Germany*

(Received 1 September 2006; published 27 November 2006)

The excitation energies and electric multipole decay rates of the lowest lying $2^+$ and $3^-$ vibrational states in Pb, Sn, and Ni nuclei are calculated following relativistic quasiparticle random-phase approximation formalism based on the relativistic Hartree-Bogoliubov mean field. Two sets of Lagrangian parameters, NL1 and NL3, are used to investigate the effect of the nuclear force. Overall there is good agreement with the available experimental data for a wide range of mass numbers considered here, and the NL3 set seems to be a better choice. However, strictly speaking, these studies point toward the need of a new set of force parameters that could produce more realistic single-particle levels, at least in vicinity of the Fermi surface, of a wide range of nuclear masses.

DOI: 10.1103/PhysRevC.74.054313 PACS number(s): 21.10.Re, 21.60.Jz, 27.60.+j, 27.80.+w

## I. INTRODUCTION

The ground-state properties of finite nuclei, throughout the periodic table, have been very successfully described by relativistic mean-field models [1]. In this framework the nucleons of a nucleus are described as relativistic Dirac particles that interact by exchange of mesons, such as the isoscalar scalar $\sigma$ meson, the isoscalar vector $\omega$ meson, and the isovector vector $\rho$ meson. Electromagnetic photon fields are also considered. Various sets of interaction coupling constants—going by names such as NL1, NL3, HS, and NLSH—are considered in the literature. An effective density dependence is introduced by replacing the quadratic $\sigma$ potential term in the Lagrangian density $\frac{1}{2}m_\sigma^2\sigma^2$ with a quartic potential $U(\sigma) = \frac{1}{2}m_\sigma^2\sigma^2 + \frac{1}{3}g_2\sigma^3 + \frac{1}{4}g_3\sigma^4$. The inclusion of pairing correlations is essential for a quantitative description of open-shell nuclei. In the present scheme the aforementioned Lagrangian is used to produce the mean-field single-particle states. Then a nonrelativistic pairing potential in the particle-particle channel is added to operate between these single-particle states. We use pairing part of the Gogny finite-range interaction D1S [2,3] for this purpose. Finally, relativistic Hartree-Bogoliubov (RHB) equations are solved in a self-consistent manner.

In the nonrelativistic mean-field framework the standard approach for the description of vibrational excited states in doubly magic spherical nuclei is the random-phase approximation (RPA) or in open-shell spherical nuclei it is the quasiparticle RPA (QRPA) [4–7]. However, Ring and co-workers [8–10] have recently derived fully self-consistent relativistic RPA and QRPA equations based on the RHB mean field within the "no-sea" approximation. To be consistent with the no-sea approximation in the mean field the Dirac sea states with negative energies are included in the configuration space of the relativistic QRPA (RQRPA) equations. Thus, besides the positive-energy particle and hole ($ph$) states the negative-energy unoccupied and positive-energy hole ($ah$) states are also included to form the RPA matrix and the latter are found to have important effects on the excitation energies as well as the decay rates [9].

Recently [11], we have applied this approach to calculate the energies of the first excited $2^+$ states and corresponding $B(E2)$ decay rates for tin isotopes with even mass numbers $A = 100$–$134$ and for Pb isotopes with $A = 202$–$214$ by employing the NL3 set of the Lagrangian parameters. Overall agreement with the available experimental data is very good. In view of recent interest [12,13] in such calculations for nuclei around $^{132}$Sn, and the large value of the $B(E2)$ transition rate at $A = 132$ compared to its nearest neighboring isotopes observed by Radford *et al.* [14,15], our results in the RQRPA calculations [11] are very satisfying and encouraging.

In the present paper we would like to report on our detailed investigations on the lowest excitation energies of the $2^+$ and $3^-$ vibrational states and their decay rates $B(E; 0^+ \to 2^+)$ [briefly written as $B(E2)\uparrow$] and $B(E3)\uparrow$ in the RQRPA approach for Pb, Sn, and Ni isotopes.

In the next section we present very briefly the formalism and some calculational details. Section III contains results and discussions spread over three subsections for Pb, Sn, and Ni isotopes. Finally, a summary and conclusions are presented in Sec. IV.

## II. FORMALISM AND CALCULATION DETAILS

The mean-field approximation represents the lowest order of the quantum field theory when the meson field operators are replaced by their expectation values. The couplings of the meson fields to the nucleons are adjusted to reproduce the ground-state properties of nuclear matter and some selected finite nuclei. The $\sigma$ meson approximates a large attractive scalar field. The $\omega$ meson describes the short-range repulsion between the nucleons, and the $\rho$ meson carries the isospin quantum number, which is important for nuclei far away from the $N \sim Z$ line. In the present investigations the calculations are performed by employing two sets of Lagrangian parameters,

 ©2006 The American Physical Society

TABLE I. Parameter sets NL1 and NL3 of the effective Lagrangian used in the present calculation including the nucleon mass $m$.

| Parameter | NL1 | NL3 |
|---|---|---|
| $m$ (MeV) | 938.0 | 939.0 |
| $m_\sigma$ (MeV) | 492.25 | 508.194 |
| $m_\omega$ (MeV) | 795.359 | 782.501 |
| $m_\rho$ (MeV) | 763.0 | 763.0 |
| $g_\sigma$ | 10.138 | 10.217 |
| $g_\omega$ | 13.285 | 12.868 |
| $g_\rho$ | 4.975 | 4.474 |
| $g_2$ (fm$^{-1}$) | −12.172 | −10.431 |
| $g_3$ | −36.265 | −28.885 |

NL1 and NL3, and the results are compared with the available experimental data. The NL1 and NL3 parameter sets are listed in Table I and the parameters of the Gogny D1S interaction are listed in Table II.

Details of the derivation of fully self-consistent RQRPA equations, based on the time-dependent RHB model in a small-amplitude-oscillation approximation, can be found in Refs. [8,9]. These equations are derived in the canonical basis in which the RHB single-particle density $\rho(\vec{r}, \vec{r'})$ is diagonal, with eigenvalues $v^2$ as occupation probabilities in the BCS theory for a system with even number of particles. However, in contrast to the BCS theory, neither the Dirac Hamiltonian ($h_D$) nor the pairing fields ($\Delta$) are diagonal in this canonical representation. For spherical nuclei the RQRPA equations can be obtained for angular-momentum-coupled two-quasiparticle states. In standard notation these equations are written in matrix form as

$$\begin{pmatrix} A^J & B^J \\ -B^{*J} & -A^{*J} \end{pmatrix} \begin{pmatrix} X^{\nu J} \\ Y^{\nu J} \end{pmatrix} = \omega_\nu \begin{pmatrix} X^{\nu J} \\ Y^{\nu J} \end{pmatrix}. \tag{1}$$

For every excited phonon energy $\omega_\nu$, the quantities $(X^\nu)$ and $(Y^\nu)$ denote the forward- and backward-going two-quasiparticle amplitudes, respectively. The amplitudes $Y^\nu$ are the measure of the RPA correlations in the ground state. In the canonical basis the $A$ and $B$ matrices are given by

$$\begin{aligned} A^J_{kk'll'} = {} & H^{11(J)}_{kl}\delta_{k'l'} - H^{11(J)}_{k'l}\delta_{kl'} - H^{11(J)}_{kl'}\delta_{k'l} + H^{11(J)}_{k'l'}\delta_{kl} \\ & + \tfrac{1}{2}(\xi^+_{kk'}\xi^+_{ll'} + \xi^-_{kk'}\xi^-_{ll'})V^{pp}_{(kk'll')J} + \zeta_{kk'll'}V^{ph}_{(kl'k'l)J}, \end{aligned} \tag{2}$$

$$\begin{aligned} B^J_{kk'll'} = {} & \tfrac{1}{2}(\xi^+_{kk'}\xi^+_{ll'} - \xi^-_{kk'}\xi^-_{ll'})V^{pp}_{(kk'll')J} \\ & + \zeta_{kk'll'}(-1)^{j_l - j_{l'}+J}V^{ph}_{(klk'l')J}. \end{aligned} \tag{3}$$

TABLE II. Parameter set D1S for the effective Gogny interaction.

| $i$ | $\mu_i$ (fm) | $W_i$ | $B_i$ | $H_i$ | $M_i$ |
|---|---|---|---|---|---|
| 1 | 0.7 | −1720.3 | 1300.0 | −1813.53 | 1397.60 |
| 2 | 1.2 | 103.69 | −163.483 | 162.812 | −223.934 |

The matrix elements of the one-quasiparticle term $H^{11}$ are given by

$$H^{11}_{kl} = (u_k u_l - v_k v_l)h_{D_{kl}} - (u_k v_l + v_k u_l)\Delta_{kl}. \tag{4}$$

$V^{pp}$ and $V^{ph}$ are the residual two-body interactions in the particle-particle and particle-hole channels, respectively, and the notation $(kk'll')J$, etc. indicates $J$-coupled two-body matrix elements. The pairing factors are defined as

$$\zeta_{kk'll'} = \begin{cases} \eta^+_{kk'}\eta^+_{ll'} & \text{for } \sigma \text{ and the time components of } \omega,\ \rho, \\ & \text{and } A, \\ \eta^-_{kk'}\eta^-_{ll'} & \text{for the spacelike components of } \omega,\ \rho, \\ & \text{and } A, \end{cases}$$

with

$$\eta^\pm_{kk'} = u_k v_{k'} \pm (-1)^J v_k u_{k'} \tag{5}$$

and

$$\xi^\pm_{kk'} = u_k u_{k'} \mp v_k v_{k'}. \tag{6}$$

The reduced electric transition probability from the ground state to an excited state with angular momentum $J$ and excitation energy $\omega_\nu$ for a multipole operator $\hat{Q}^J$ is given by

$$\begin{aligned} B(E; 0 \to J, \omega_\nu) = \Bigg| & \sum_{kk'} \Big( \langle k||\hat{Q}^J||k'\rangle X^{\nu J}_{kk'} \\ & + (-1)^{j_k - j_{k'}+J}\langle k'||\hat{Q}^J||k\rangle Y^{\nu J}_{kk'} \Big) \\ & \times (u_k v_{k'} + (-1)^J v_k u_{k'}) \Bigg|^2. \end{aligned} \tag{7}$$

As already mentioned, besides the two-quasiparticle configurations built from the positive-energy states, the RQRPA configuration space also includes the pair configurations formed from positive-energy and empty negative-energy states from the Dirac sea. Since in the relativistic case the matrix $A$ has large negative diagonal elements, the RPA eigenvalue equations cannot be reduced to a Hermitian problem of half the dimension, even if the matrix elements are real. Thus, one has to diagonalize a non-Hermitian matrix with large dimensions. In practice the matrix dimension is fixed by using maximum cutoff energies, $E_{ph}$ and $E_{ah}$. We have fixed these to $E_{ph} = 140$ MeV and $E_{ah} = 1800$ MeV. As an illustration, we show in the following for the case of $^{208}$Pb how $E_2$, $B(E2)$, $E_3$, and $B(E3)$ change with $E_{ah}$. The dependence of $E_2$ (left-hand-side scale) and $B(E2)$ (right-hand-side scale) on $E_{ah}$ is displayed in Fig. 1 for the number of basis oscillator shells $N_f = 12$, 14, and 20 with the use of the NL3 set of the Lagrangian parameters. For $N_f = 20$ and $E_{ah} = 2000$ MeV the dimension becomes more than 4000 and calculation has not been done for this point on the figure. Similarly, the dependence of $E_3$ and $B(E3)$ on $E_{ah}$ is displayed in Fig. 2. The dependence of these quantities on $E_{ph}$ (not discussed here) is fixed to be 140 MeV by following similar investigations. It is evident from both figures that for $E_{ah} \geqslant 1800$ MeV good convergence is reached. As for convergence in the basis space, $N_f > 14$ seems to be quite satisfactory. We take $N_f = 16$ for the present calculations.

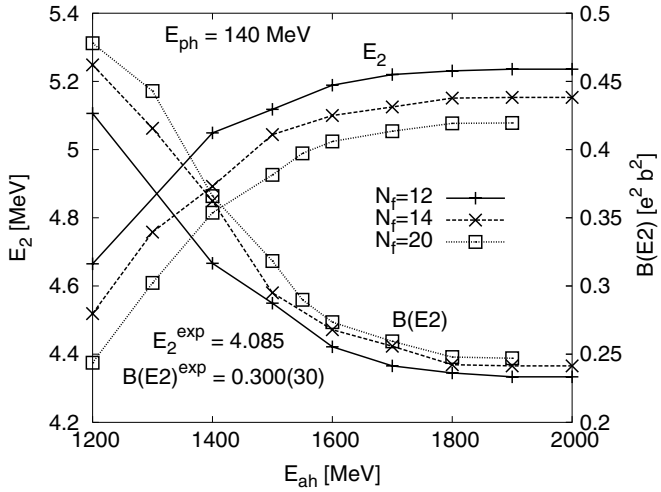


FIG. 1. Excitation energy $E_2$ and $B(E2)\uparrow$ decay rates of $^{208}$Pb with NL3 set of parameters as a function of the cutoff in the maximum of antiparticle-hole energy $E_{ah}$ with basis space defined by the number of oscillator shells, $N_f = 12$, 14, and 20. The experimental values are also shown to highlight the difference from the computed numbers.

## III. RESULTS AND DISCUSSIONS

In the present investigation the energy and decay rates of the first excited vibrational quadrupole ($2^+$) and octupole ($3^-$) states have been calculated for the even-mass isotopic chains of Pb, Sn, and Ni nuclei by employing NL1 and NL3 sets of the Lagrangian parameters in the RQRPA model. For the convenience of systematic discussion of our findings the results are presented in separate sections for each isotopic chain of these nuclei.

### A. Pb isotopes

The calculations are performed for $A = 194$–$212$ even-mass isotopes. The Pb nuclei with $A < 194$ and $A > 212$ turn out to be quadrupole deformed in the ground state in RHB calculations [10], with $A = 194$ and 212 nuclei being actually the border cases. In Fig. 3 we display the variation of $E_2$ (in MeV) as a function of $A$. With both NL1 and NL3 forces the agreement with the experimental data [16] is quite reasonable. For the same mass range the $B(E2)\uparrow$ transition rates are compared with the available experimental data [16] in Fig. 4, and the agreement is excellent. Furthermore, at least for $^{204-210}$Pb, the agreement is slightly better with the NL1 force.

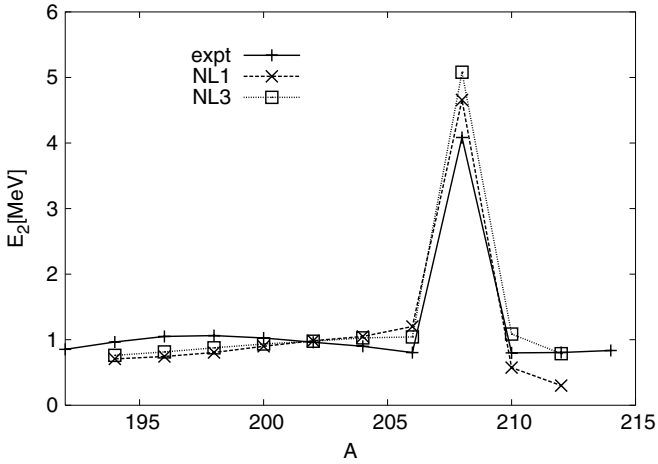


FIG. 3. Energy $E_2$ of Pb isotopes calculated with the parameter sets NL1 and NL3 compared with available experimental data as a function of $A$.

To analyze qualitatively the relative contributions of protons and neutrons to the lowest $2^+$ excitations in these nuclei we show in Fig. 5 their separate contributions to the RQRPA wave function normalization $\sum_{i,j}(X_{ij}^2 - Y_{ij}^2) = 1$ for each isotope. It is seen that, as expected from $B(E2)$ rates, except at $A = 208$, the contribution of protons ($I_p$) is very small compared to that of neutrons ($I_n$). At $A = 208$ the shell gaps in proton and neutron single-particle spectra at the Fermi levels lead to comparable contributions from both types of the nucleons,

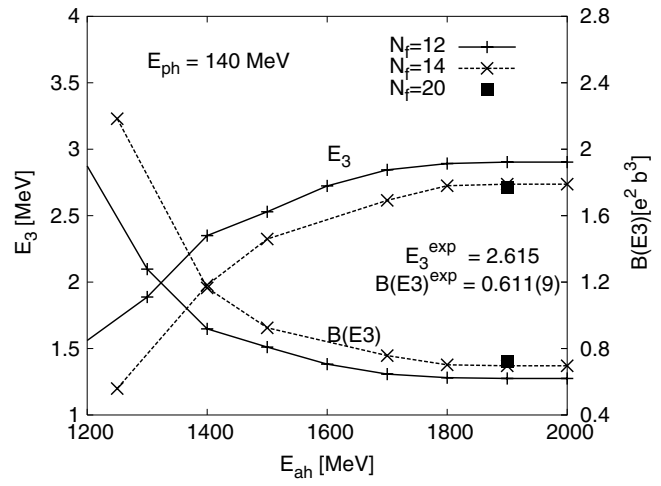


FIG. 2. Same as Fig. 1 for the excitation energy $E_3$ and decay rates $B(E3)\uparrow$. However, for $N_f = 20$ only one point at $E_{ah} = 1900$ MeV is shown.

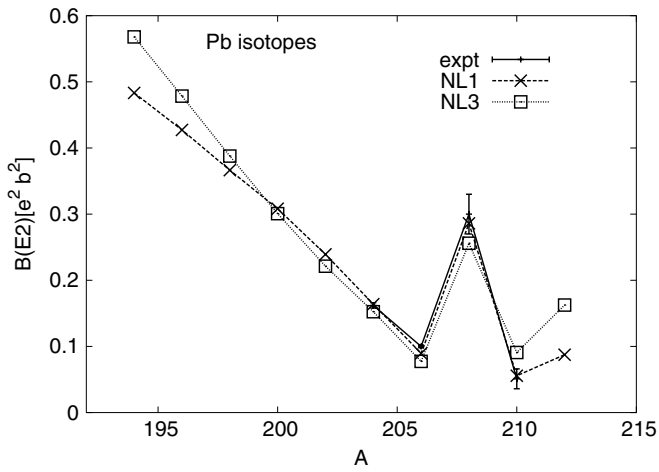


FIG. 4. Same as Fig. 3 for the $B(E2)\uparrow$ rates.

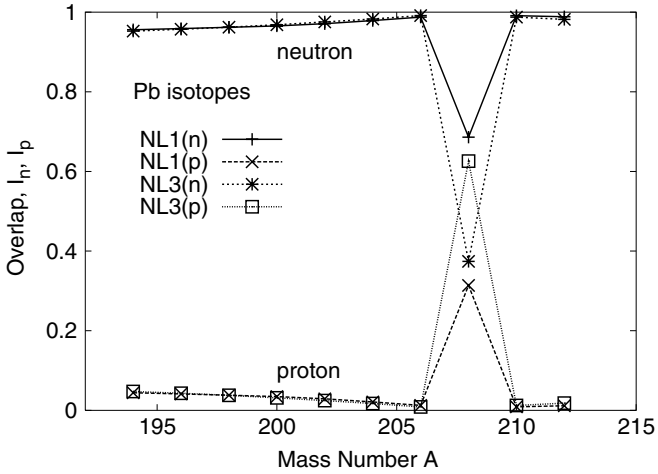


FIG. 5. Contributions of neutrons ($I_n$) and protons ($I_p$) to the QRPA wave function overlap unity as a function of $A$ for Pb.

leading to enhanced $B(E2)$ transition rates compared to that for its immediate neighbors (see also [11]).

Now in Figs. 6 and 7 we display the variation of $E_3$ and $B(E3)\uparrow$, respectively, as a function of $A$. Here the agreement with the available experimental data [17] is not as good as that for the $2^+$ states. The NL3 force appears reasonable compared to NL1 for $E_3$, whereas for $B(E3)$, NL1 seems to do better with a sudden drop in the value at $A = 210$. But the range of $A$ for which data are available is rather small for more serious quantitative conclusions. Particularly, for $A < 204$ the availability of the data on $B(E2)$ as well as on $B(E3)$ would be very useful for the theoretical analysis. In view of the good agreement between theory and experiment on $E_2$, it would be of interest to compare with the experimental data the predicted gradual, rather steep, increase of $B(E2)$ rates (increase in quadrupole collectivity) with the decrease of $A$. Whereas the excitation energy $E_2$ for the isotopes with $A = 194$–$206$ is of the order of an MeV, these calculations predict $E_3$ as steeply increasing with an increase of $A$ for the same mass range.

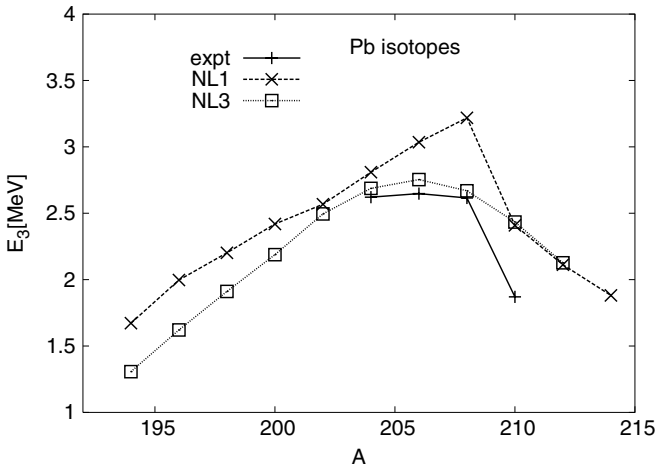


FIG. 6. Same as Fig. 3 for energy $E_3$.

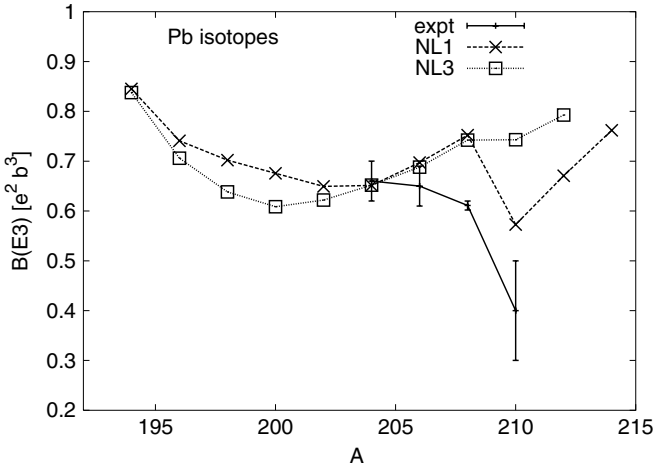


FIG. 7. Same as Fig. 6 for $B(E3)\uparrow$.

### B. Sn isotopes

Recently [11], we have already studied the structural properties of the first excited $2^+$ states of even-mass $A =$ 100–134 Sn isotopes by employing the NL3 force parameters in RQRPA. In the present study these calculations are repeated for all these isotopes by using the NL1 set of parameters. Then the quantities $E_3$ and $B(E3)$ are calculated with both these parameter sets. The variation of $E_2$ with $A$ is displayed in Fig. 8. On the figure the label SM indicates results of a large-scale shell-model calculation [18] performed for $A =$ 102–130 found by taking $^{100}$Sn as an inert core with the basis space spanned by the spherical orbitals ($g_{7/2}, d, s, h_{11/2}$). An effective neutron charge $e_n = 1.0\ e$ is required for an overall fit to the $B(E2)$ data. Whereas the experimental and SM values of $E_2$ are almost constant around a value of 1.2 MeV for $A =$ 102–130, the RQRPA ones with the NL3 force show a good agreement with these with a small oscillatory behavior matching almost exactly at $A = 118$. However, the magnitude of such an oscillatory nature becomes rather large with NL1 parameters, resulting in a poor agreement with the data for

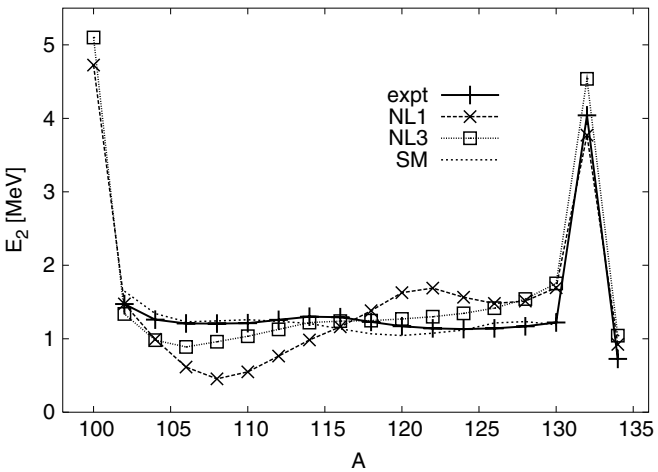


FIG. 8. Energy $E_2$ as a function of $A$ for Sn isotopes calculated with NL1 and NL3 force parameters compared with available experimental data and shell-model results.

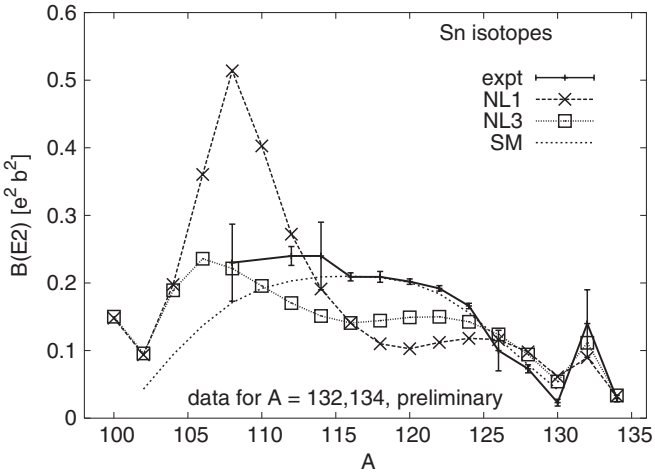


FIG. 9. Same as Fig. 8 for the $B(E2)\uparrow$ transition rates.

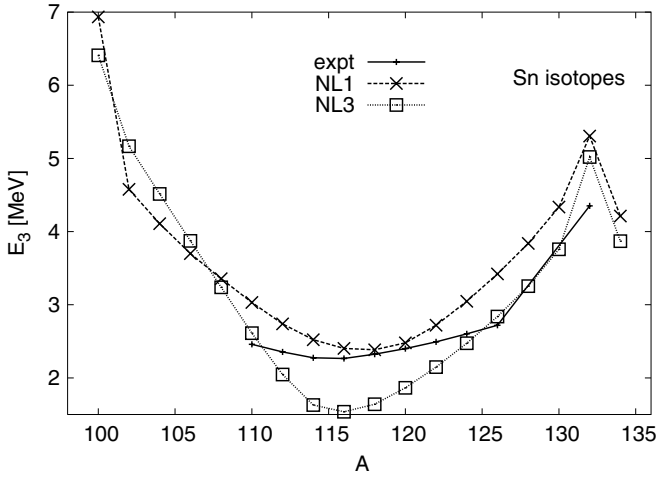


FIG. 11. Same as Fig. 8 for energy $E_3$.

most of the isotopes. The agreement with the data is good for $A = 132$ and 134 with both forces. For $^{100}$Sn we predict $E_2 \approx 5.0$ MeV.

The dependence of $B(E2)$ on $A$ is shown in Fig. 9. The RQRPA results (labeled NL1, NL3) can be compared with the available experimental data [14–16,18] and shell-model (SM) results [18]. We notice that the SM results follow an inverted parabolic pattern with maximum collectivity at the mid-shell nucleus $^{116}$Sn and minimum near the doubly magic shell closures. The SM results agree very well with the experimental data for $A = 116$–130, and underestimate it for $A < 116$, implying the importance of the effect of core polarization of the doubly magic nucleus $^{100}$Sn [18]. In this sense it is very satisfying that the RQRPA results show the enhancement of $B(E2)$ with the decrease of $A$ with a maximum around $A = 106$. Though the two parameter sets give rise to similar results at and near $^{100}$Sn and $^{132}$Sn, the NL1 results are not good for most of the nuclei in the intermediate-mass range. The NL3 results are in overall very good agrement with the data. Figure 10 shows (as in Fig. 5) the separate neutron ($I_n$) and proton ($I_p$) contributions to the QRPA wave function overlap normalized to unity. At $A = 100$ and 132 the sudden rise of the proton contributions explains the jump of $B(E2)$ values at these mass numbers.

The calculated excitation energies $E_3$ and decay rates $B(E3)\uparrow$ are compared with available data [17] in Figs. 11 and 12, respectively. We observe that, in contrast to that for $E_2$ and $B(E2)$, here $E_3$ and $B(E3)$ computed with the NL1 force parameters are relatively in a better agreement with the data than those computed with the use of NL3. Another point to note is that variation of both the quantities $E_3$ and $B(E3)$ with $A$ shows roughly a parabolic shape between the mass numbers 102 and 130. The extremum points lie close to the mid-shell nucleus. We find that overall agreement of the $E_2$ and $B(E2)$ with the data is better with the use of the NL3 force, and that of $E_3$ and $B(E3)$ is better with the use of the NL1. Thus, these investigations (studying the dynamic properties) have brought to light new challenges regarding the fixing of the force parameters.

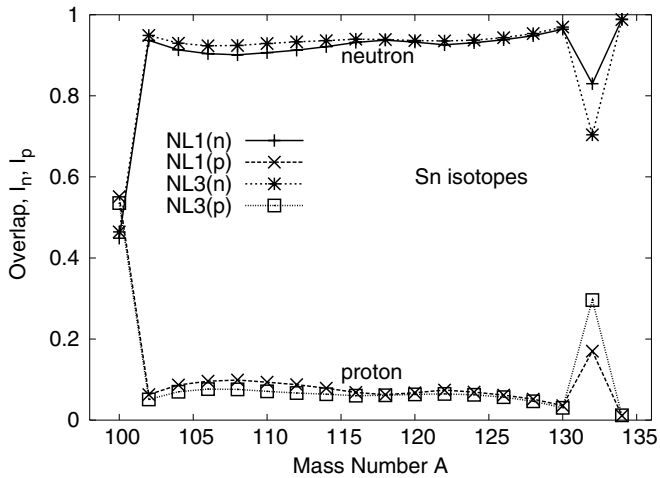


FIG. 10. Same as Fig. 5 for Sn isotopes.

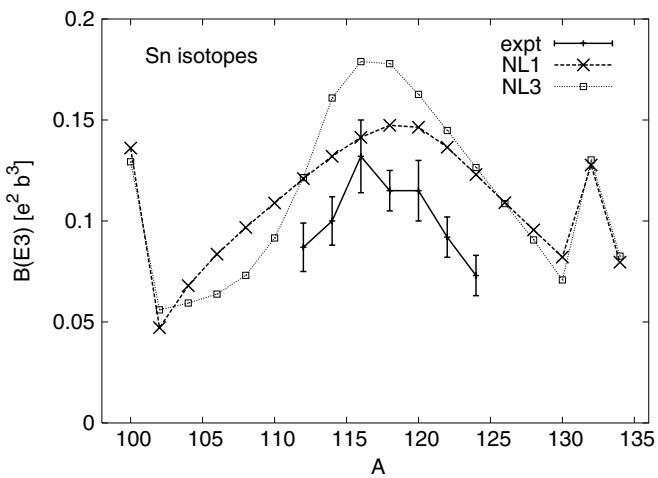


FIG. 12. Same as Fig. 11 for the $B(E3)\uparrow$ transition rates.

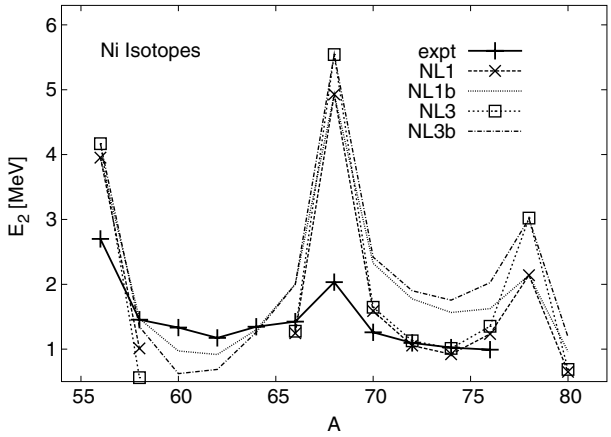


FIG. 13. Energy $E_2$ as a function of mass number compared with available experimental data for the Lagrangian parameter sets NL1 and NL3. For $A = 60$–64 the QRPA eigenvalues turn out to be imaginary or very small real numbers and are omitted from the plot. The curves labeled NL1b and NL3b correspond to NL1 and NL3 forces, respectively, but with a stronger pairing interaction when all the pairing channel matrix elements are multiplied by an overall factor $V_{\text{fac}} = 1.15$.

### C. Ni isotopes

The isotopic chain of even-mass Ni nuclei considered here has $A = 56$–80, showing variation of the ratio $N/Z = 1$ to 1.86. In this mass range there are three doubly magic Ni nuclei, with $N = 28$, 40, and 50. This is clearly reflected from the experimental data on $E_2$ [16,19] and $B(E2)$ [16,20–22] at $N = 28$ and 40, as seen in Figs. 13 and 14, respectively. At $A = 68$ the calculated value of $E_2$ is about a factor of 3 too large compared to the data value. This reflects on the importance of the $np$-$nh(n \geqslant 2)$ type of excitations from the $pf$ shell to the $g_{9/2}$ orbitals. As Fig. 13 shows, there are four theoretical curves labeled NL1, NL3, NL1b, and NL3b. The latter two labels refer to the case when the pairing channel matrix elements of the Gogny-D1S interaction are overall multiplied by a constant factor, $V_{\text{fac}} = 1.15$. Corresponding to NL1 and NL3 the RPA eigenvalues for $A = 60$–64 turn out to be imaginary or very small real numbers (about 0.2–0.3 MeV) and so these points are omitted on the plot. These are the signs of instability of the mean-field solutions for these nuclei. However, with the enhanced pairing interaction strength these become real, though still smaller than the data values at $A = 60$ and 62. For the heavier isotopes, $A = 70$–76, there is a good agreement with the experimental data [16,19] as the curves labeled NL1 and NL3 indicate. However, the enhancement of the pairing interaction strengths (NL1b, NL3b) increases the $E_2$ values, as expected, and spoils the aforementioned good agreement for the heavier isotopes. That is, such an increase in pairing interaction strength is desirable only for the lighter isotopes of Ni (as is also the case for Sn).

The variation of $B(E2)$ as a function of $A$ is displayed in Fig. 14. The symbols on the figure have meanings similar to those of Fig. 13. As expected, when the $E_2$ energies are too small, the $B(E2)$ values are too large and vice versa, except at and close to the shell closures. The recently observed [22] $B(E2) \uparrow = 0.0860 \pm 0.0140\ e^2\,\text{b}^2$ for $^{70}$Ni is not reproduced here as well as in predictions of Ref. [23]. In shell-model calculations of Ref. [24] for $A = 70$–76 the $B(E2)$ value at $A = 70$ can be reproduced only with the use of a free effective neutron charge $e_n \geqslant 1.5\ e$, as can be seen in the figure here. (With $e_n = 1.0\ e$, as reported in [24], agreement is much worse than that obtained by us.) We do predict a parabolic shape for the $B(E2)$ rates between $A = 70$ and 78 without any free parameter. Also, in magnitude these appear to be reasonable for $A > 70$.

Figure 15 exhibits the variation of $E_3$ as a function of $A$. Experimental data [17] are known only for $A = 56$–66 and show a monotonic decrease with increasing $A$. The theoretical curves with NL1 as well as NL3 forces show a similar, somewhat steeper, trend with a minimum at $A = 68$ and an overall conical shape between $A = 56$ and 78. The calculated number at $A = 56$ is too high ($\sim$10.0 MeV) and is not shown in the figure. It seems to be a good coincidence that at $A = 58$ and 78 both forces produce almost the same value.

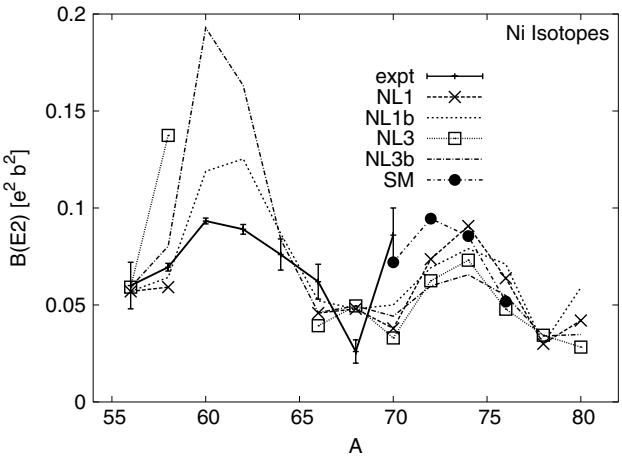


FIG. 14. Same as Fig. 13 for the $B(E2) \uparrow$ transition rates. The shell-model (SM) results for $A = 70$–76 are with a quadrupole effective neutron charge $e_n = 1.5\ e$ [24].

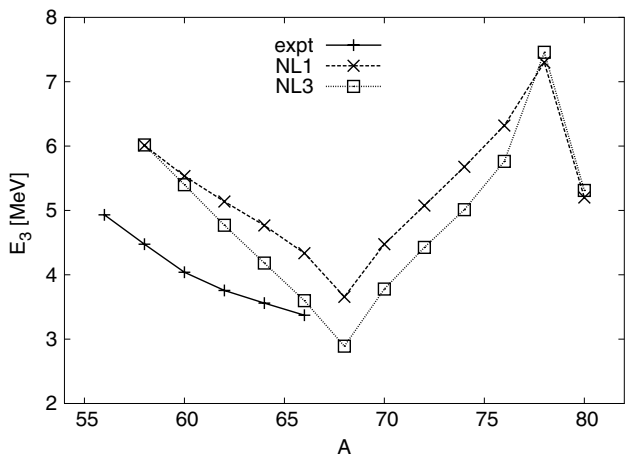


FIG. 15. Same as Fig. 11 for Ni isotopes. For $A = 56$ the value of $E_3$ is about 10.0 MeV with both NL1 and NL3.

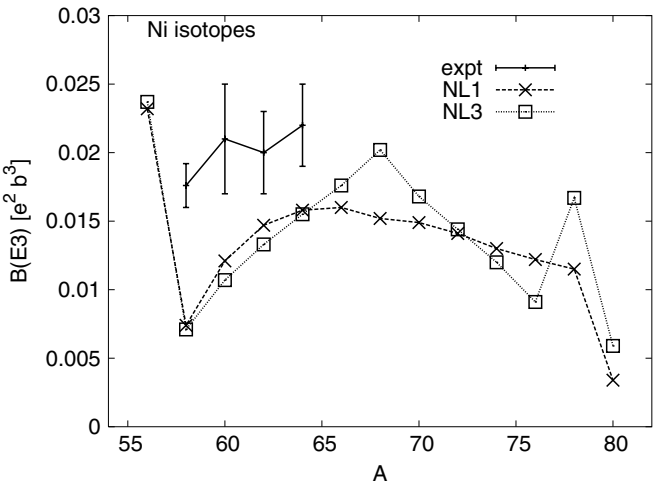


FIG. 16. Same as Fig. 15 for the $B(E3)\uparrow$ transition rates.

The $B(E3)\uparrow$ results shown in Fig. 16 are more or less consistent with the variation of $E_3$ with $A$. At and around $A = 78$ the $B(E3)$ values with the use of the NL3 force seem to be more realistic. An increase of the pairing interaction strength (e.g., $V_{\text{fac}} = 1.15$) has little effect on the values of $E_3$ and $B(E3)$.

## IV. SUMMARY AND CONCLUSIONS

The excitation energies and decay rates of the first excited $2^+$ and $3^-$ vibrational states of several Pb, Sn, and Ni isotopes have been studied in the RQRPA approach by employing NL1 and NL3 sets of the Lagrangian parameters. For the particle-particle pairing channel the nonrelativistic Gogny D1S interaction has been used. Overall a quite satisfactory agreement with the available experimental data is obtained for a wide mass range without any adjustable free parameter in the theory.

However, we do find some inconsistencies: For example, the $E_2$ and $B(E2)$ values of Sn isotopes as a function of mass number are better reproduced with the use of NL3 force parameters, whereas the $E_3$ and $B(E3)$ values favor the use of NL1. Therefore, more studies like the present ones are needed to fine-tune the Lagrangian parameters. Also more complete experimental information on neutron-deficient and neutron-rich isotopes would be helpful for theoretical models. Next we are planning to calculate the magnetic dipole moments of the lowest $2^+$ states in Sn and Ni isotopes as these are even more sensitive to the orbitals near the Fermi surface.

Recently, a new effective interaction, DD-ME2, with explicit density dependence of the nucleon-meson couplings has been developed [25]. It would be desirable to repeat the present RQRPA calculations by employing this new set of force parameters.

## ACKNOWLEDGMENT

This work has been supported in part by the Bundesministrium für Bildung und Forschung under Project No. 06MT246.

[1] P. Ring, Prog. Part. Nucl. Phys. **37**, 193 (1996).
[2] J. F. Berger *et al.*, Comput. Phys. Commun. **61**, 365 (1991).
[3] T. Gonzalez-Llaren, J. L. Egido, G. A. Lalazissis, and P. Ring, Phys. Lett. **B379**, 13 (1996).
[4] K. F. Liu and G. E. Brown, Nucl. Phys. **A265**, 385 (1976).
[5] J. P. Blaizot and D. Gogny, Nucl. Phys. **A284**, 429 (1977).
[6] J. Dechargé and D. Gogny, Phys. Rev. C **21**, 1568 (1980).
[7] N. Van Giai and H. Sagawa, Nucl. Phys. **A371**, 1 (1981).
[8] P. Ring, Z. Ma, N. Van Giai, D. Vretenar, A. Wandelt, and L. Cao, Nucl. Phys. **A694**, 249 (2001).
[9] N. Paar, P. Ring, T. Niksic, and D. Vretenar, Phys. Rev. C **67**, 034312 (2003).
[10] D. Vretenar, A. V. Afnasjev, G. A. Lalazissis, and P. Ring, Phys. Rep. **409**, 101 (2005).
[11] A. Ansari, Phys. Lett. **B623**, 37 (2005).
[12] J. Terasaki, J. Engel, W. Nazarewicz, and M. Stoitsov, Phys. Rev. C **66**, 054313 (2002).
[13] S. Sarkar and M. S. Sarkar, Eur. Phys. J. A **21**, 61 (2004).
[14] D. C. Radford *et al.*, Nucl. Phys. **A746**, 83c (2004).
[15] J. R. Beene *et al.*, Nucl. Phys. **A746**, 471c (2004).
[16] S. Raman, C. W. Nestor Jr., and P. Tikkanen, At. Data Nucl. Data Tables **78**, 1 (2000).
[17] T. Kibedi and R. H. Spear, At. Data Nucl. Data Tables **80**, 44 (2002).
[18] A. Banu *et al.*, Phys. Rev. C **72**, 061305(R) (2005).
[19] C. Mazzocchi *et al.*, Phys. Lett. **B622**, 45 (2005).
[20] S. Leenhardt *et al.*, Eur. Phys. J. A **14**, 1 (2002).
[21] O. Sorlin *et al.*, Phys. Rev. Lett. **88**, 092501 (2002).
[22] O. Perru *et al.*, Phys. Rev. Lett. **96**, 232501 (2006).
[23] K. Langanke, J. Terasaki, F. Nowacki, D. J. Dean, and W. Nazarewicz, Phys. Rev. C **67**, 044314 (2003).
[24] A. Lisetsky, B. A. Brown, M. Horoi, and H. Grawe, Phys. Rev. C **70**, 044314 (2004).
[25] G. A. Lalazissis, T. Niksic, D. Vretenar, and P. Ring, Phys. Rev. C **71**, 024312 (2005).